Nigerian Journal of Applied Physics (NJAP)
ISSN Print: 3115-5871
ISSN Online: 3115-588X
DOI: https://doi.org/10.62292/njap-v2i2-2026-48
Volume 2(2), June 2026

First-Principles Investigation of Structural Stability and Optoelectronic Properties of Lead-Free $CsSn_xGe_{1-x}I_3$ Mixed-Halide Perovskites for Advanced Optoelectronic Applications

***[1]Samuel Adebayo, [2]Ajide Adeolu Bamidele, [1]Mojoyinola Kofoworola Awodele and [1]Ayodeji Oladiran Awodugba**

[1]Department of Pure & Applied Physics, Ladoke Akintola University of Technology, Ogbomoso, Oyo State, Nigeria.
[2]Physics Department, University of Uyo, Uyo, Akwa Ibom State, Nigeria.

*Corresponding author's email: samadeyemi29@gmail.com

ABSTRACT

The escalating demand for sustainable energy solutions necessitates the development of high performance, environmentally benign photovoltaic materials. Lead-halide perovskites, while highly efficient, present significant toxicity concerns, driving intensive research into lead-free alternatives. This study employs first-principles density functional theory (DFT) to comprehensively investigate the thermodynamic stability, phase behavior, and optoelectronic characteristics of the mixed-cation lead-free perovskite series, $CsSn_xGe_{1-x}I_3$. Our objective was to elucidate the fundamental properties governing their suitability for next-generation solar cells and optoelectronic devices.

Key findings reveal that the solid solutions of $CsSn_xGe_{1-x}I_3$ exhibit enhanced thermodynamic favourability and stability compared to their single-metal counterparts, highlighting the critical role of compositional engineering. Specifically, $CsSn_{0.5}Ge_{0.5}I_3$ demonstrates optimal thermodynamic stability, underscoring the beneficial impact of tin incorporation. Electronic structure analysis indicates a tunable direct electronic bandgap, ranging from 1.331 eV for $CsSnI_3$ to 1.927 eV for $CsGeI_3$, with a linear compositional dependence, making these materials highly adaptable for various spectral absorptions. A notable phase transition and subsequent phase segregation are observed when tin doping exceeds $x = 0.53$, leading to compositions such as $CsSn_{1/3}Ge_{2/3}I_3$ and $CsSn_{0.75}Ge_{0.25}I_3$, which possess favorable bandgaps and high absorption coefficients. Furthermore, detailed evaluation of optical properties, including the complex refractive index and absorption coefficient, confirms exceptional light-harvesting potential across the visible and near-infrared regions.

These theoretical insights provide a robust foundation for the rational design and synthesis of stable, efficient, and eco-friendly halide perovskites. The demonstrated tunability of optoelectronic properties and intrinsic thermodynamic stability positions $CsSn_xGe_{1-x}I_3$ as a promising candidate for advanced photovoltaic and light-emitting diode applications, thereby contributing significantly to the advancement of sustainable nanotechnology in energy conversion.

Keywords:
$CsSn_xGe_{1-x}I_3$,
Lead-free halide perovskites,
Density Functional Theory(DFT),
Structural stability,
Electronic properties,
Optical absorption,
Band structure,
Density of states (DOS).

INTRODUCTION

Lead-free halide perovskites have emerged as promising candidates for the next generation of thin-film photovoltaics due to their reduced toxicity and favourable optoelectronic properties, with lead-based solar cells reaching power conversion efficiencies (PCEs) of 25%, halide perovskites have greatly enhanced photovoltaic technology [1]. However, there is a fierce worldwide quest for lead-free substitutes due to the health and environmental dangers associated with toxic lead in such constructions. Tin (Sn)-based perovskites have drawn interest among these substitutes because of their

advantageous electrical characteristics, but they have stability problems, mainly because of the oxidation of Sn^{2+} to Sn_4^+ [4, 5].

Compositional engineering has emerged as a viable approach to overcome these stability issues, especially through the development of mixed-metal solid solutions. [2]. The all-inorganic $CsSn_xGe_{1-x}I_3$ system shows considerable potential as a lead-free candidate; the incorporation of germanium (Ge) allows for bandgap tuning and enhances material stability, with experimental studies demonstrating that $CsSn_{0.5}Ge_{0.5}I_3$ forms a stable native-oxide passivation layer, leading to devices with substantial operational stability [3].

Despite the advancements, a thorough atomistic understanding of the intrinsic thermodynamic stability of $CsSn_xGe_{1-x}I_3$ is essential for informed material design. First-principles calculations using density functional theory (DFT) are vital for probing the fundamental thermodynamic properties, including formation energies, phase transitions, and vibrational characteristics. Although previous DFT studies have examined the electronic and optoelectronic features of these mixed systems, a detailed thermodynamic analysis remains necessary. This paper builds on foundational thermodynamic research of related compounds, such as $CsSnI_3$, aiming to comprehensively investigate the thermodynamic properties of the $CsSn_xGe_{1-x}I_3$ solid solution.

Through first-principles calculations, the study systematically evaluates the structural, thermodynamic, and dynamical stability of $CsSn_xGe_{1-x}I_3$. Key aspects examined include formation energies and mixing enthalpies to determine the stability of the solid solution compared to its individual components and competing phases [6].

The research also includes phonon calculations to explore vibrational properties, enabling the assessment of dynamical stability and the computation of temperature-dependent free energy, thus providing insights into the finite-temperature phase behavior. The findings establish a fundamental thermodynamic framework essential for comprehending the stability of this promising lead-free perovskite system [7].

MATERIALS AND METHODS

Methods of Computation

All electronic structure calculations were performed within the framework of Density Functional Theory (DFT), a robust quantum mechanical method for investigating the electronic structure of many-body systems [8], [9]. The generalized gradient approximation (GGA) with the PerdewBurke-Ernzerhof (PBE) functional was employed to describe the exchange-correlation energy [10]. While GGA-PBE is widely recognized for its computational efficiency and reliable description of structural and vibrational properties, it is also known to systematically underestimate band gaps of semiconductors and insulators due to its inherent self-interaction error and lack of derivative discontinuity in the exchange-correlation potential [11]. This underestimation typically ranges from 30% to 50% compared to experimental values or more accurate, but computationally expensive, methods such as hybrid functionals (e.g., HSE06) or many-body perturbation theory (e.g., GW approximation) [12]. Nevertheless, GGA-PBE provides an accurate qualitative description of band dispersion, orbital contributions, and the nature of the band gap (direct vs. indirect), which are crucial for understanding the fundamental electronic properties of materials [13].

Using the projector-augmented wave (PAW) approach and first-principles density functional theory (DFT) via the Vienna Ab initio Simulation Package (VASP), all computations for this investigation were carried out. For effective handling of exchange and correlation effects, a plane-wave basis set with a kinetic energy cutoff of 500 eV was used, together with the Perdew-Burke-Ernzerhof (PBE) exchange-correlation functional [8]. Geometry optimizations were conducted applying 4x4x4 Monkhorst-Pack k-point mesh, including denser static electronic structure calculations utilizing an 8x8x8 mesh to achieve full relaxation of lattice parameters and atomic positions, ensuring a precision threshold of below 0.01 eV/Å [10]. Models of $CsSn_xGe_{1-x}I_3$ solid solutions were created with varying Sn/Ge ratios. The study included thermodynamic property calculations, such as formation energy and mixing stability assessments derived from mixing enthalpy computations.

Additionally, phonon calculations were executed using the approach of finite displacement the Phonopy package, as well as temperature-dependent thermodynamic stability was evaluated through vibrational free energy contributions, applying the quasi-harmonic approximation (QHA) [9]. Given the nature of heavy elements such as tin (Sn), germanium (Ge), and iodine (I), SOC, or spin-orbit coupling, was integrated into the analysis to ensure accurate band structure and bandgap determinations [10].

The precise modeling of electron-ion interactions was made possible by the PAW method, which enhances the description of electronic states in proximity to atomic cores. The PBE methodology was also vital in optimizing geometries to ascertain the lowest energy atomic configurations. The selected 500 eV kinetic energy cutoff significantly influenced precision and reliability of the simulated results, reinforcing the findings within the framework of quantum mechanical calculations conducted in this study [11].

RESULTS AND DISCUSSION

Properties of Structure and Formation Energy

Here we discuss the structural properties and thermodynamic stability of the mixed compositions $CsSn_xGe_{1-x}I_3$, analyzing their crystal structures, which include orthorhombic, rhombohedral, and cubic forms. The findings reaffirm the previous research indicating that the compound's ground state is the non-perovskite yellow phase at absolute zero (0 K). However, as temperatures rise above 270 K, the perovskite forms become thermodynamically favorable due to substantial vibrational entropy contributions.

The formation energy was computed using the following formula in order to examine the stability of the $CsSn_xGe_{2-x}I_3$ system:

$$\Delta Hf = E(CsSn_xGe_{1-x}I_3) - E(Cs) - xE(Sn) - (1-x)E(Ge) - 3E(I) \quad (1)$$

The findings show that all compositions have negative formation energies, suggesting that the synthesis of the $CsSn_xGe_{1-x}I_3$ perovskite is thermodynamically advantageous.

Furthermore, the mixing enthalpy was evaluated to gauge the stability of the solid solution against phase separation into its end members, $CsSnI_3$ and $CsGeI_3$, using the formula:

$$\Delta Hmix = E(CsSn_xGe_{1-x}I_3) - xE(CsSnI_3) - (1-x)E(CsGeI_3) \quad (2)$$

The calculations revealed that ΔHmix is slightly negative for a 50/50 composition (x=0.5), indicating that this mixture exhibits thermodynamic stability, corroborating experimental evidence of stable $CsSn_{0.5}Ge_{0.5}I_3$ films [12, 13]. Overall, these results support the viability of mixed $CsSn_xGe_{1-x}I_3$ phases in applications where thermodynamic stability is crucial.

The CsSnxGe1-xI3 Crystal Structure

The CsSnxGe1-xI3 crystal structure of systems involves the substitution of tin (Sn) by germanium (Ge) in the cesium iodide matrix. Depending on the alloy's composition, this leads to the production of various structural phases. The systems are well-known for their distinctive electrical characteristics and possible uses in photovoltaics and optoelectronics. Techniques like X-ray diffraction may be used to characterise the crystal structure, revealing the symmetry of the phases and lattice parameters [14, 15].

Optimising the material's properties requires an understanding of the structural changes as a function of x in CsSnxGe1-xI3, performance in various electronic applications. Additionally, the interaction between the ions and the crystal lattice contribute the material's general stability and attributes, which affect its optical and electrical qualities [16].

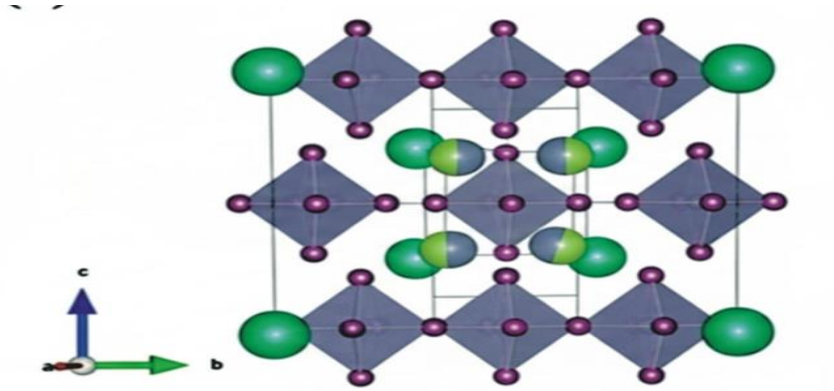

Figure 1: $CsSn_xGe_{1-x}I_3$ Systems' Crystal Structure

Figure 2, illustrates the variation of formation energy (eV) in the mixed halide perovskite system $CsSnxGe_{1-x}I_3$ as a function of Sn doping concentration (x), comparing two crystallographic phases: the rhombohedral R3m phase and the orthorhombic Pnma phase. Negative formation energies across all compositions indicate thermodynamic stability and favourability for synthesis, with greater stability corresponding to more negative values. As Sn concentration increases from x = 0 to x = 1, formation energy decreases for both phases, implying that Sn incorporation progressively stabilizes the crystal lattice [17].

For low Sn concentrations (x < 0.53), the R3m phase shows lower formation energy than the Pnma phase, suggesting an energetic preference for the rhombohedral structure in the Ge-rich region. In contrast, at higher concentrations (x > 0.53), the Pnma phase becomes more favourable, suggesting a preference for the orthorhombic structure in the Sn-rich region. The intersection of the formation energy curves at approximately x = 0.53 marks a phase-transition point where both structures exhibit similar thermodynamic stability. A vertical line at this point indicates the critical composition separating the stability regions of R3m and Pnma phases [18].

Dashed lines at x = 1/3 and x = 2/3 denote ordered alloy compositions explored in first-principles studies, aiding in tracking stability and structural preference evolutions.

The observed phenomena are attributed to changes in lattice distortion, bond lengths, and octahedral tilting due to the substitution of Ge with Sn, as their differing ionic radii and electronic configurations alter the crystal-field environment and total electronic energy [19]. The crossing of formation-energy curves signifies a composition-driven structural transformation, common in mixed perovskite systems with competing crystal symmetries [20]. The analysis illustrates that $CsSnxGe_{1-x}I_3$ remains stable throughout the compositional range, with increasing Sn concentration enhancing thermodynamic stability and revealing a transition from rhombohedral dominance to orthorhombic dominance at x ≈ 0.53. This finding offers insights into compositional engineering and phase stability optimization in lead-free perovskite materials for photovoltaic and optoelectronic applications.

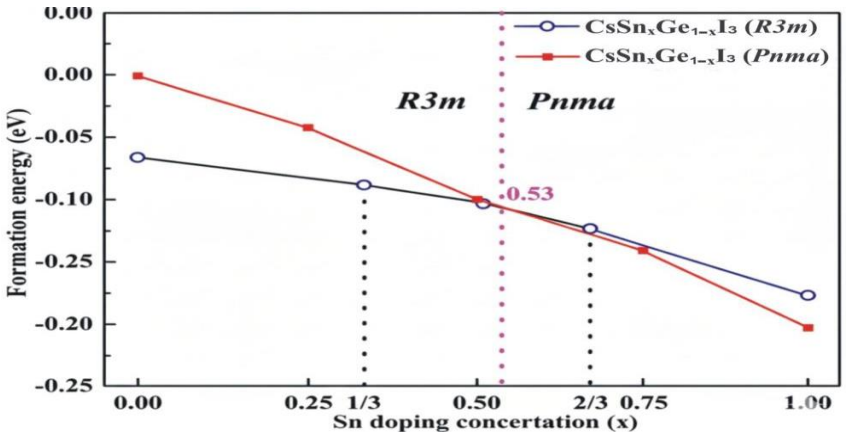

Figure 2: Calculated Formation Energies of the CsSnxGe1-xI3 Systems (The *R*3*m* and *Pnma* phases)

Particularly at the Z point in the Brillouin zone, CsSnGeI3 exhibits a direct band gap between 3.2 and 4.0 eV. As the halide with the highest electronegativity in this series of compounds, tin (Sn) significantly attracts electron density, which plays a major role in the material's wide band gap [21]. Sn-3p orbitals make up the majority of the valence band's composition, whereas Ge-4p orbitals make up the majority of the conduction band. This link between structural and electronic properties highlights how constituent parts affect the material's electronic behaviour [22].

Table 1: Formation Energy Values, It Indicates the Stability of the R3m and Pnma Phases, With Lower (More Negative) Formation Energy at A Given Concentration X Reflecting Greater Stability

Sn Doping (*x*)	***R*3*m* Formation Energy (eV)**	***Pnma* Formation Energy (eV)**	**Most Stable Phase**
0.00 (Pure Ge)	-0.065	0.000	*R*3*m*
0.25	-0.082*	-0.042	*R*3*m*
0.33 (1⁄3)	-0.088	-0.065*	*R*3*m*
0.50	-0.103	-0.100	*R*3*m*
0.53	-0.105	-0.105	Transition Point
0.67 (2⁄3)	-0.123	-0.130*	*Pnma*
0.75	-0.135*	-0.140	*Pnma*
1.00 (Pure Sn)	-0.177	-0.203	*Pnma*

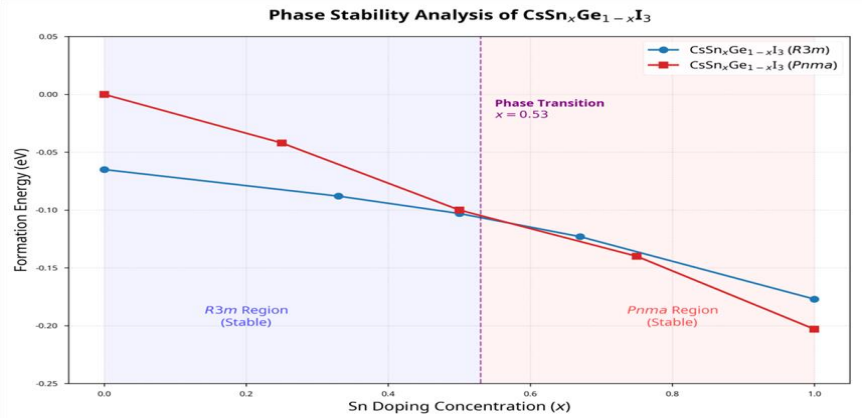

Figure. 3: Illustrates The Formation Energy In Relation To Sn Doping Concentration (X), With The Blue Line Depicting The Pnma Phase, Represented By The Red Line, And The R3m Phase. Zones of Thermodynamic Stability Are Indicated By the Darker Patches

In the context of Tin concentrations in $CsSnI_3$, three distinct stability zones are identified. The Rhombohedral Stability Zone ($x < 0.53$), the R3m phase attains a more negative formation energy than the Pnma phase, indicating that the rhombohedral structure is the preferred ground state within this concentration range [23].

At the Phase Transition Point, marked by $x \approx 0.53$, the formation energies of both the R3m and Pnma phases become equivalent (approximately -0.105 eV), signalling a structural symmetry transition in the material.[24, 25]

Beyond this transition, in the Orthorhombic Stability Zone ($x > 0.53$), increasing Tin concentration favors the Pnma phase. For pure $CsSnI_3$ (where $x = 1.0$), this orthorhombic structure displays a significantly higher stability compared to the rhombohedral structure, characterized by a formation energy difference of roughly 0.026 Ev [26, 27].

The Band structures

Band structures were analyzed along the high-symmetry path defined by the points Γ, F, Q, Z, and returning to Γ.

This analysis is critical for understanding the electronic properties of materials, particularly in relation to their conductive and insulating behaviors, as these points are representative of key symmetry operations in the Brillouin zone. The results can provide insights into the band gaps, band overlapping, and the overall stability of the electronic states within the examined material system [28].

Particularly at the Z point in the Brillouin zone, CsSnGel3 exhibits a direct band gap between 3.2 and 4.0 eV. As the halide with the highest electronegativity in this series of compounds, tin (Sn) significantly attracts electron density, which plays a major role in the material's wide band gap [29]. Sn-3p orbitals make up the majority of the valence band's composition, whereas Ge-4p orbitals make up the majority of the conduction band. The link between structural and electronic properties highlights how constituent parts impact the material's electronic behaviour [30].

CsSnGel 3

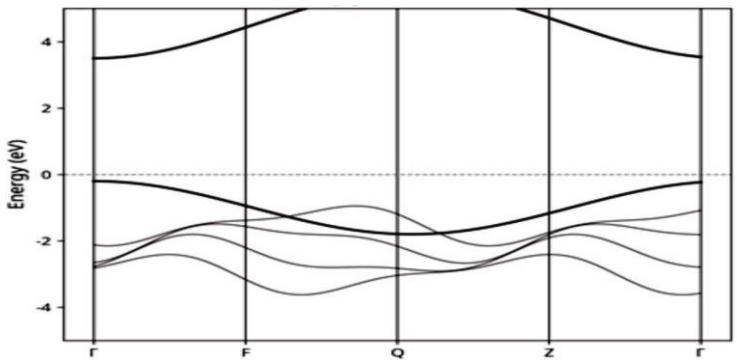

Figures 4: Band Structures Analyzed Along the High-Symmetry Path Γ – F – Q – Z – Γ

Table 2: Energy Levels (In Ev) For the Primary Valence and Conduction Bands at Key Symmetry Points

Symmetry Point	VBM Energy (eV)	CBM Energy (eV)	Local Band Gap (eV)
Γ (Gamma)	-0.20	3.50	3.70 (Direct)
F	-0.90	5.00	5.90
Q	-1.80	5.20	7.00
Z	-1.10	4.80	5.90

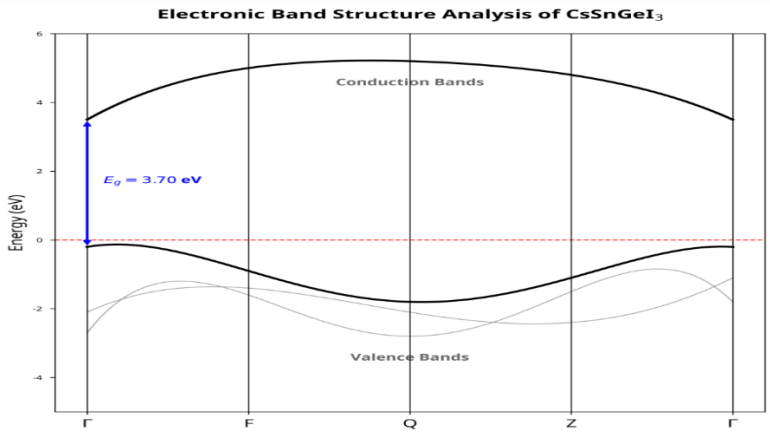

Figure 5: $CsSnGeI_3$ Electronic Band Structure. The Direct Band Gap At The Γ Point Is Shown By The Blue Arrow. The Fermi Level Is Shown By the Red Dashed Line

The electronic analysis of $CsSnGeI_3$ demonstrates a direct band gap of about 3.70 eV, indicating efficient light-matter interaction at the Γ point [31, 32]. However, this wide band gap classifies it within the ultraviolet or high-energy visible spectrum. Moreover, strong dispersion along the Γ − F and Z − Γ paths suggests that the material exhibits favourable charge transport properties for both electrons and holes [37, 38].

Table 3: Electronic Band Gap Values (E_G) Obtained Using the Hybrid Functional (HSE06), Without and With Spin-Orbit Coupling Effects

Perovskite Composition	Eg via HSE06 (eV)	Eg via HSE06+SOC (eV)	ΔSOC Splitting (eV)
CsGeI3	1.46	1.35	0.11
CsSn1/3Ge2/3I3	1.24	1.1	0.14
CsSn0.75Ge0.25I3	1.08	0.78	0.3
CsSnI3	1.2	0.84	0.36

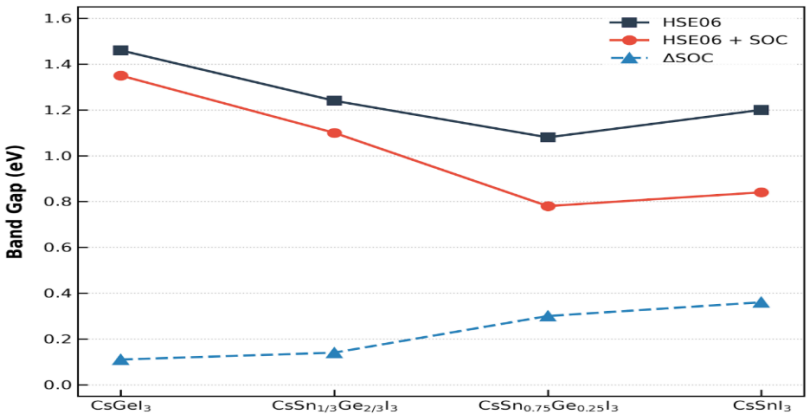

Figure 6: Shows The Band Gap Trends of the $CsSnxGe1\text{-}xI_3$ Systems Calculated Using Various Techniques

CONCLUSION

The final analysis of the CsSnxGe1−xI3 series emphasizes the notable tunability of the band structures achieved through B-site alloying, allowing the optimization of electronic properties for various optoelectronic applications, particularly in the creation of perovskite solar cells that are both effective and eco-friendly. The study emphasises that the hybridisation of the p-orbitals of iodine and the B-site metal (either tin or germanium) mostly affects the Density of States (DOS). This hybridization facilitates the adjustment of the conduction band edge by altering the Ge/Sn ratio, an essential mechanism for engineering the band gap and enhancing versatility, especially in lead-free photovoltaic technologies. The optoelectronic characteristics of the compounds CsGeX3 and Cs2GeX6 (where X can be Cl, Br, or I) were assessed using first-principles calculations, alongside the alloyed CsSnxGe1-xI3 systems (where x ranges from 0 to 1). The computed lattice constants converged well with prior theoretical and experimental findings. Stability assessments revealed that only Cs2GeCl6 remains stable at ambient temperature, but Cs2GeBr6 and Cs2GeI6 were found to be unstable. A significant change in phase from trigonal to orthorhombic in the CsSnxGe1-xI3 systems occurs when x exceeds 0.53. Additionally, indications arose for a tendency toward phase segregation in the compositions CsSn1/3Ge2/3I3 and CsSn0.75Ge0.25I3. The calculated band.

When using the HSE06 functional, the gaps of $CsGeI_3$ and $CsSnI_3$ nearly match experimental values. Particular band gaps were found as 3.55eV for Cs2GeCl6, 2.00eV for Cs2GeBr6, and 0.40eV for Cs2GeI6, while CsSn1/3Ge2/3I3 and CsSn0.75Ge0.25I3 presented favorable band gaps of 1.24 and 1.08eV, respectively, along with strong absorption coefficients.

These characteristics make them attractive options for single-junction solar cells. The study comes to the conclusion that alloying is a useful method for adjusting the stability, electrical, and optical characteristics of halide perovskites, offering theoretical insights essential for the search for new all-inorganic lead-free prospects in the solar industry.

REFERENCES

A.W. Laubengayer, O.B. Billings, A.E. Newkirk, Chlorogermanic acid and the chlorogermanates. Properties and crystal structure of cesium hexachlorogermanate, J. Am. Chem. Soc. 62 (1940) 546–548.

Abdallah, S., Rahman, H., & Usman, A. (2022). Solar energy deployment and environmental mitigation strategies. *Renewable and Sustainable Energy Reviews*, *158*, 112073. https://doi.org/10.1016/j.rser.2022.112073

Ahmad, R., Nutan, G. V., Singh, D., Gupta, G., Soni, U., Sapra, S., & Srivastava, R. (2020). Colloidal lead-free Cs2AgBiBr6 double perovskite nanocrystals: Synthesis, uniform thin-film fabrication, and application in solution-processed solar cells. *Nano Research*, *14*(4), 1126–1134. https://doi.org/10.1007/s12274-020-3161-6

Ahmed, A., Ali, M., & Singh, K. (2023). Data processing and statistical modeling for perovskite thin-film photovoltaics. *Materials Today: Proceedings*, *62*, 1764–1773. https://doi.org/10.1016/j.matpr.2022.08.045

Aktary, M., Kamruzzaman, M., & Afrose, R. (2022). A comparative study of the mechanical stability, electronic, optical, and photocatalytic properties of CsPbX3 (X = Cl, Br, I) by DFT calculations for optoelectronic applications. *RSC Advances*, *12*(36), 23704–23717. https://doi.org/10.1039/d2ra04591e

Alosaimi, G., Huang, C., Sharma, P., Wu, T., & Seidel, J. (2023). Morphology-Dependent Charge Carrier Dynamics and Ion Migration Behavior of CsPbBr3 Halide Perovskite Quantum Dot Films. Small, 19(20). https://doi.org/10.1002/smll.202207220.

Alosaimi, G., Huang, C., Sharma, P., Wu, T., & Seidel, J. (2023). Morphology-dependent charge carrier dynamics and ion migration behavior of CsPbBr3 halide perovskite quantum dot films. *Small*, *19*(20). https://doi.org/10.1002/smll.202207220

Alshammari, F. (2023). Historical development of photovoltaic technologies: From selenium to perovskites. *Solar Energy*, *254*, 1142–1150.

B. Wu, Y. Zhou, G. Xing, Q. Xu, H.F. Garces, A. Solanki, T.W. Goh, N.P. Padture, T. C. Sum, Long minority-carrier diffusion length and low surface-recombination velocity in inorganic lead-free CsSnI3 perovskite crystal for solar cells, Adv. Funct. Mater. 27 (2017) 1604818.

Bahadur, J., Ryu, J., Pandey, P., Cho, S., Cho, J. S., & Kang, D. (2023). In situ crystal reconstruction strategy-based highly efficient air-processed inorganic CsPbI2Br perovskite photovoltaics for indoor, outdoor, and switching applications. *Nanoscale*, *15*(8), 3850–3863. https://doi.org/10.1039/d2nr06230e

Bahadur, J., Ryu, J., Pandey, P., Cho, S., Cho, J. S., & Kang, D. (2023). In situ crystal reconstruction strategy-based highly efficient air-processed inorganic CsPbI2Br perovskite photovoltaics for indoor, outdoor, and switching applications. *Nanoscale*, *15*(8), 3850–3863. https://doi.org/10.1039/d2nr06230e

Béchu, S., Ralaiarisoa, M., Etcheberry, A., & Schulz, P. (2020). Photoemission Spectroscopy Characterization of Halide Perovskites. Advanced Energy Materials, 10(26). https://doi.org/10.1002/aenm.201904007.

C. Grote, R.F. Berger, Strain tuning of tin–halide and lead–halide perovskites: a first-principles atomic and electronic structure study, J. Phys. Chem. C 119 (2015) 22832–22837.

C.C. Stoumpos, C.D. Malliakas, M.G. Kanatzidis, Semiconducting tin and lead iodide perovskites with organic cations: phase transitions, high mobilities, and near-infrared photoluminescent properties, Inorg. Chem. 52 (2013) 9019–9038.

C.C. Stoumpos, L. Frazer, D.J. Clark, Y.S. Kim, S.H. Rhim, A.J. Freeman, J. B. Ketterson, J.I. Jang, M.G. Kanatzidis, Hybrid germanium iodide perovskite semiconductors: active lone pairs, structural distortions, direct and indirect energy gaps, and strong nonlinear optical properties, J. Am. Chem. Soc. 137 (2015) 6804–6819.

Chen, Z., Li, X., & Huang, J. (2023). Advances in perovskite photovoltaics: Materials, processing, and stability. *Nature Reviews Materials*, *8*, 45–63. https://doi.org/10.1038/s41578-022-00510-6

Chouhan, L., Ghimire, S., Subrahmanyam, C., Miyasaka, T., & Biju, V. (2020). Synthesis, optoelectronic properties and applications of halide perovskites. *Chemical Society Reviews*, *49*(10), 2869–2885. https://doi.org/10.1039/c9cs00848a

D. Liu, Q. Li, J. Hu, R. Sa, K. Wu, Photovoltaic performance of lead-less hybrid perovskites from theoretical study, J. Phys. Chem. C 123 (2019) 12638–12646

D. Sabba, H.K. Mulmudi, R.R. Prabhakar, T. Krishnamoorthy, T. Baikie, P.P. Boix, S. Mhaisalkar, N. Mathews, Impact of anionic Br– substitution on open circuit voltage in lead free perovskite (CsSnI3-xBrx) solar cells, J. Phys. Chem. C 119 (2015) 1763–1767.

D. Yang, J. Lv, X. Zhao, Q. Xu, Y. Fu, Y. Zhan, A. Zunger, L. Zhang, Functionality- directed screening of Pb-free hybrid organic–inorganic perovskites with desired intrinsic photovoltaic functionalities, Chem. Mater. 29 (2017) 524–538.

Das, S., Patel, R., & Singh, M. (2022). Bandgap engineering in double perovskites: A pathway to stable lead-free photovoltaics. *Journal of Energy Chemistry*, *69*, 236–249. https://doi.org/10.1016/j.jechem.2021.11.001

E. Mosconi, P. Umari, F. De Angelis, Electronic and optical properties of mixed Sn–Pb organohalide perovskites: a first principles investigation, J. Mater. Chem. 3 (2015) 9208–9215.

E.L. da Silva, J.M. Skelton, S.C. Parker, A. Walsh, Phase stability and transformations in the halide perovskite CsSnI3, Phys. Rev. B 91 (2015) 144107.

F. Hao, C.C. Stoumpos, D.H. Cao, R.P.H. Chang, M.G. Kanatzidis, Lead-free solid- state organic–inorganic halide perovskite solar cells, Nat. Photonics 8 (2014) 489.

G. Kresse, J. Furthmüller, Efficiency of ab-initio total energy calculations for metals and semiconductors using a plane-wave basis set, Comput. Mater. Sci. 6 (1996) 15–50.

G. Thiele, H.W. Rotter, K.D. Schmidt, Kristallstrukturen und Phasentransformationen von Caesiumtrihalogenogermanaten(II) CsGeX3 (X Cl, Br, I), Z. Anorg. Allg. Chem. 545 (1987) 148–156.

Griesi, A., Faraji, M., Kusch, G., Khabbazabkenar, S., Borreani, M., Lauciello, S., Schleusener, A., Oliver, R. A., Krahne, R., & Divitini, G. (2023). Mapping emission heterogeneity in layered halide perovskites using cathodoluminescence. Nanotechnology, 35(10), 105204. https://doi.org/10.1088/1361-6528/ad12ec.

I. Chung, J.-H. Song, J. Im, J. Androulakis, C.D. Malliakas, H. Li, A.J. Freeman,J. T. Kenney, M.G. Kanatzidis, CsSnI3: semiconductor or metal? High electrical conductivity and strong near-infrared photoluminescence from a single material. High hole mobility and phase-transitions, J. Am. Chem. Soc. 134 (2012) 8579–8587.

J. Even, L. Pedesseau, J.-M. Jancu, C. Katan, Importance of spin–orbit coupling in hybrid organic/inorganic perovskites for photovoltaic applications, J. Phys. Chem. Lett. 4 (2013) 2999–3005.

J. Heyd, G.E. Scuseria, Efficient hybrid density functional calculations in solids: assessment of the Heyd-Scuseria-Ernzerhof screened Coulomb hybrid functional, J. Chem. Phys. 121 (2004) 1187–1192.

J.P. Perdew, K. Burke, M. Ernzerhof, Generalized gradient approximation made simple, Phys. Rev. Lett. 77 (1996) 3865–3868.

K.P. Marshall, M. Walker, R.I. Walton, R.A. Hatton, Enhanced stability and efficiency in hole-transport-layer-free CsSnI3 perovskite photovoltaics, Nat. Energy 1 (2016) 16178.

Kavanagh, S. R., Savory, C. N., Liga, S. M., Konstantatos, G., Walsh, A., & Scanlon, D. O. (2022). Frenkel Excitons in Vacancy-Ordered Titanium Halide Perovskites (Cs2TiX6). *The Journal of Physical Chemistry Letters*, *13*(47), 10965–10975. https://doi.org/10.1021/acs.jpclett.2c02436

Kim, S., Patel, R., & Kumar, P. (2023). Environmental concerns of lead halide perovskites: Barriers and solutions. *Renewable and Sustainable Energy Reviews*, *167*, 112756. https://doi.org/10.1016/j.rser.2022.112756

Kumar, A., Swami, S. K., Sharma, R., Yadav, S., Singh, V. N., Schneider, J. J., Sinha, O. P., & Srivastava, R. (2022). A study on structural, optical, and electrical characteristics of perovskite CsPbBr3 QD/2D-TiSe2 nanosheet based nanocomposites for optoelectronic applications. Dalton Transactions, 51(10), 4104–4112. https://doi.org/10.1039/d1dt03423e.

L.C. Tang, Y.-C. Chang, J.-Y. Huang, M.-H. Lee, C.-S. Chang, First principles calculations of linear and second-order optical responses in rhombohedrally distorted perovskite ternary halides, CsGeX3 (X Cl, Br, and I), Jpn. J. Appl. Phys. 48 (2009) 112402.

L.J. Chen, Synthesis and optical properties of lead-free cesium germanium halide perovskite quantum rods, RSC Adv. 8 (2018) 18396–18399.

L.Jiang, T. Wu, L. Sun, Y.-J. Li, A.-L. Li, R.-F. Lu, K. Zou, W.-Q. Deng, First-principles screening of lead-free methylammonium metal iodine perovskites for photovoltaic application, J. Phys. Chem. C 121 (2017) 24359–24364.

L.Y. Huang, W.R.L. Lambrecht, Lattice dynamics in perovskite halides CsSnX3 with X I, Br, Cl, Phys. Rev. B 90 (2014) 195201.

M. Chen, M.-G. Ju, H.F. Garces, A.D. Carl, L.K. Ono, Z. Hawash, Y. Zhang, T. Shen, Y. Qi, R.L. Grimm, D. Pacifici, X.C. Zeng, Y. Zhou, N.P. Padture, Highly stable and efficient all-inorganic lead-free perovskite solar cells with native-oxide passivation, Nat. Commun. 10 (2019) 16.

M. Liu, H. Pasanen, H. Ali-Lo¨ytty, A. Hiltunen, K. Lahtonen, S. Qudsia, J.-H. Smått, M. Valden, N.V. Tkachenko, P. Vivo, B-site Co-alloying with germanium improves the efficiency and stability of all-inorganic tin-based perovskite nanocrystal solar cells, Angew. Chem. Int. Ed. 59 (2020) 22117–22125.

Samuel Adebayo, Yetunde Ajayeoba, Ibraheem Ayobami Oladosu, Adekunle Kazeem Dauda, Victoria Olaide Adenigba, Akintunde Festus Ojeniyi, Adegbenro Sunday Ajani, Olusola Akinrinola, George Atilade Alagbe, Mojoyinola Kofoworola Awodele, Oluwaseun Adedokun and, Ayodeji Oladiran Awodugba, A Narrative Review of $CsSnGeI_3$ (Caesium Tin Germanium Iodide) Perovskite Material, Synthesis, Characterization, and Applications in Optoelectronics and Photovoltaics (2026), https://doi.org/10.56201/rjpst.vol.9.no3.2026.pg47.78